Published in IET Communications
Received on 16th November 2008
Revised on 19th April 2009
doi: 10.1049/iet-com.2008.0659

ISSN 1751-8628

Equalisation of SIMO-OFDM systems with insufficient cyclic prefix in doubly selective channels

M. Beheshti M.J. Omidi A.M. Doost-Hoseini

Department of Electrical and Computer Engineering (ECE), Isfahan University of Technology (IUT), Isfahan, Iran
E-mail: m.beheshti@ec.iut.ac.ir

Abstract: Time variations of a doubly selective wireless channel and insufficient cyclic prefix (CP) length of an orthogonal frequency division multiplexing (OFDM) transmission system cause intercarrier interference (ICI) and interblock interference (IBI) as significant limitations. This paper investigates the problem of joint ICI and IBI mitigation in single-input multiple-output OFDM (SIMO-OFDM) systems. It is assumed, unlike most existing literature, that the channel delay spread is larger than the CP, and also the channel varies on each OFDM block. First, doubly selective channel is modelled using basis expansion model (BEM) and a closed-form expression for signal-to-interference-plus-noise ratio (SINR) is derived. Then, a time-domain equaliser is developed, which maximises the SINR for all subcarriers. Moreover, a frequency-domain equalisation approach is proposed which is based on the MSE minimisation per tone. A low-complexity implementation of the per-tone equaliser is also derived. An important feature of the proposed equalisers is that no bandwidth expansion or redundancy insertion is required except for the CP. Finally, complexity comparison and simulation results over Rayleigh fading channel are provided to illustrate the effectiveness of the proposed approaches. Since both equalisers are designed in the frequency domain, they provide significant interference cancellation.

1 Introduction

Orthogonal frequency division multiplexing (OFDM) has been an efficient underlying technology for wireless communications [1, 2]. OFDM is being commercially applied in wireless local area networks (IEEE 802.11a and HIPERLAN/2), terrestrial digital audio broadcasting (DAB-T) and terrestrial digital video broadcasting (DVB-T). It is the modulation of choice for the most recent IEEE 802.16 wireless metropolitan area networks. OFDM is also considered for the IEEE 802.20 mobile broadband wireless access standard currently under development and for the ultra wideband (UWB) standard under the multi-band OFDM alliance [3]. In OFDM, the computationally efficient fast Fourier transform (FFT) is used to transmit data in parallel over a large number of orthogonal subcarriers. For time-invariant (TI) frequency selective channels, when an adequate number of subcarriers are used in conjunction with a cyclic prefix (CP) of appropriate length, subcarrier orthogonality is maintained and a simple one-tap equaliser is employed to compensate for the channel distortions. In many wireless applications, however, time selectivity of the channel and insufficient CP length can lead to a loss of subcarrier orthogonality and therefore degrade the high performance of simple data detection mechanism in the conventional OFDM.

Time variations of a channel usually come from the mobility or residual frequency offsets between transmitter and receiver. If the OFDM block time duration is smaller than the channel coherence time, the channel can be approximated as constant in a block. This assumption reduces the equaliser to a one-tap filter. The channel variations within an OFDM block will lead to a loss of subcarrier orthogonality and result in interchannel

interference (ICI). The channel fading under this circumstance becomes doubly (time and frequency) selective. Time selectivity depends on the Doppler spread of the channel and the OFDM block length. Furthermore, the insufficient CP leads to interblock interference (IBI) which again results in ICI, as the original blocks cannot be reconstructed by means of a simple one-tap equaliser. An insufficient CP can arise for various reasons. A system might consciously shorten or omit the CP in order to improve the spectral efficiency. Another case is when a system operates in a range of delay spreads larger than what it is designed for. Finally, for many systems, the length of the CP is a tradeoff between the desire to eliminate IBI and to retain spectral efficiency. In other words, a CP should not be chosen to cope with the worst-case channel situation, as this would decrease the spectral efficiency [4]. The motivation of this paper is to jointly cope with ICI (because of the intrablock channel variations) and IBI (because of the insufficient CP) for applications, such as digital video broadcasting (DVB), where both of them are present.

The issue of interference cancellation and equalisation for OFDM systems has been addressed extensively in the literature and different approaches have been proposed including time-domain equalisation, frequency-domain equalisation, self-interference cancellation, turbo equalisation and polynomial cancellation coding. In [5, 6] authors propose an efficient time-domain equaliser (TEQ) based on tail cancellation and cyclic reconstruction. In a similar approach, channel shortening is used to make the effective impulse response shorter than the CP [7]. A time-domain windowing approach to restrict ICI support in conjunction with iterative minimum mean-square error (MMSE) estimation is presented in [8]. In [9, 10] matched-filter, least-squares (LS) and MMSE receivers incorporating all subcarriers are proposed. Frequency-domain symbol detection considering the constant number of dominant neighbouring subcarriers have been discussed in [11, 12]. Le *et al.* [13] introduce a method to adaptively determine the number of dominant neighbouring subcarriers within each OFDM block. Self-interference-cancellation technique is brought up in [14, 15]. In this approach, the information is modulated onto a group of subcarriers, which leads to a strong reduction in self-interference. This technique is very effective for the mitigation of ICI but reduces the spectral efficiency. In [16, 17] frequency-domain redundancy or unused subcarriers is used to eliminate the ICI. Most of these works, however, assume a sufficient CP and, hence, lack of IBI. The ICI caused by channel variations within an OFDM block is also ignored in some of these works. In other words, none of the above-mentioned attempts considers IBI in conjunction with ICI. Moreover, in this literature, the time-varying channel matrix (or an estimation of it) is required to design the equaliser, which in return, requires a large number of parameters to be identified (tracked).

In this paper, the problem of mitigating interference in single-input multiple-output (SIMO) OFDM systems over doubly selective channels is investigated. It is assumed, in contrast to most previous works, that the CP length is smaller than the maximum delay spread of the channel, and simultaneously, the channel varies on each OFDM block. Furthermore, basis expansion model (BEM) is used to approximate the time-variant (TV) channel and it is assumed that only the channel state information (CSI) in the form of BEM coefficients is available at the receiver which is more practical to obtain [18]. These coefficients are then used to design the equaliser for the true channel. In addition, a new exact formulation for signal-to-interference-plus-noise ratio (SINR) at the output of the FFT demodulator is derived. Based on this formulation, a time-domain linear equaliser is proposed, which maximises the SINR for all subcarriers. This TEQ is actually designed in the frequency domain. The channel shortening equaliser (pre-filter) proposed in [7] is also based on SINR maximisation. However, it uses a different SINR formulation which only takes into account the insufficient CP in a TI channel. So, it is different from the TEQ of this paper. Moreover, a per-tone frequency-domain equalisation approach is proposed, where each separate tone is equalised based on a linear MMSE equaliser design. A low-complexity implementation of the per-tone equaliser (PTEQ) is also derived.

Similarly, Barhumi *et al.* [19] uses BEM and introduces two methods for equalisation of OFDM over doubly selective channels whose delay spread is larger than the CP. However, there are main differences between its equalisation methods and what is proposed here:

- The TV finite-impulse-response (TV-FIR) TEQ designed in [19] is based on minimising MSE between the outputs of TEQ and a target impulse response. This equaliser is designed in the time domain and is basically different from the TEQ proposed in this paper.

- While Barhumi *et al.* [19] derives a frequency-domain PTEQ by transferring the TEQ operation to the frequency domain, the PTEQ proposed here is designed directly in the frequency domain. The only interpretation expressed in [19] for PTEQ method is that it is the result of transferring a TEQ to the frequency domain; however, this paper presents a clear interpretation for our proposed PTEQ as a two-dimensional interference cancellation scheme.

- The PTEQ of [19] has different structures for different values of BEM frequency resolution (to be defined later), whereas the PTEQ proposed here uses a single structure with less complexity for different BEM resolutions, yielding the same BER performance. The detailed comparison of these approaches is presented in next sections.

The remainder of this paper is organised as follows. In Section 2, the system model as well as a new ICI and IBI analysis for SIMO-OFDM is presented. In Section 3, the

TEQ is designed. In Section 4, per-tone frequency-domain equalisation is described and an efficient implementation of the proposed PTEQ is presented. Section 5 discusses the complexity of the proposed approaches. In Section 6, the unification property of the proposed equalisers is shown. In Section 7, the bit error rate (BER) performance of the proposed algorithms is illustrated through computer simulations. Section 8 concludes the paper.

Notation: Column vectors are typeset in bold lowercase, whereas matrices are in bold uppercase. $\mathcal{E}\{\cdot\}$ represents the expectation operator. The Kronecker product is denoted by $\otimes$. The transpose, Hermitian and complex conjugate operators are represented by $(\cdot)^{\mathrm{T}}$, $(\cdot)^{\mathrm{H}}$ and $(\cdot)^*$, respectively. The mth entry of vector $\boldsymbol{a}$ is shown as $\boldsymbol{a}_m$. A diagonal matrix with $\boldsymbol{a}$ on the diagonal is denoted as $\mathrm{diag}\{\boldsymbol{a}\}$. The pseudo-inverse of matrix $\boldsymbol{B}$ is denoted by $\boldsymbol{B}^{\dagger}$. N is the FFT/IFFT size; $\boldsymbol{\mathcal{F}}$ stands for unitary FFT matrix of size N; k is a tone index in a multicarrier array; the kth FFT row is $\boldsymbol{\mathcal{F}}^{(k)}$; c is the CP length; i is the OFDM block time index. The $m \times m$ identity matrix is denoted as $\boldsymbol{I}_m$. The $m \times p$ all-zero matrix is represented by $\boldsymbol{0}_{m\times p}$.

2 System model and interference analysis

In this section, first, the model used for transceiver and channel is described. Then, ICI and IBI at the receiver are formulated. The system under consideration is depicted in Fig. 1. A single-input multiple-output channel model with N_r receive antennas (or oversampling the received signal by a factor of N_r) is assumed, but the extension of the results to MIMO system is straightforward. At the transmitter, the data stream is divided into blocks of length N. For each block, the inverse IFFT is applied to convert the data into the time domain. Then, a cyclic prefix of length c is added to each block. The time-domain blocks are then serially transmitted over a time and frequency-selective channel. At the receiver, the CP is removed and time- or frequency-domain equalisation as well as FFT demodulation is performed to extract the transmitted blocks. Suppose $x_k[i]$ is the QPSK symbol transmitted on the kth subcarrier in the ith OFDM block. The transmitted time-domain sequence $u[n]$ can then be written as

$$u[n] = \frac{1}{\sqrt{N}} \sum_{k=0}^{N-1} x_k[i] \mathrm{e}^{\mathrm{j}2\pi mk/N} \tag{1}$$

where $i = \lfloor n/(N+c) \rfloor$, and $m = n - i(N+c) - c$. Note that this description includes the transmission of a CP of length c. Considering the baseband-equivalent description and assuming symbol rate sampling, the received sequence at the rth receive antenna is written as

$$y^{(r)}[n] = \sum_{\theta=-\infty}^{+\infty} h^{(r)}[n;\, \theta] u[n-\theta] + \xi^{(r)}[n] \tag{2}$$

where $\xi^{(r)}[n]$ is additive noise, and $h^{(r)}[n;\, \theta]$ is the equivalent baseband impulse response of the doubly selective channel, which is comprised of the physical channel as well as the transmit and receive filters. The noise is assumed to be a zero-mean white complex Gaussian process that is independent of the transmitted sequence.

In this paper, the doubly selective channel is modelled using BEM. Different kinds of BEM have been introduced in the literature [20–23]. This study uses the BEM of [21, 23], which has been shown to accurately model realistic channels. In this BEM, the channel is modelled as a TV FIR filter, where each tap is expressed as a superposition of complex exponential basis functions with frequencies on an FFT grid. Assuming the channel Doppler spread is bounded by $f_{\max}$, it is possible to accurately model the doubly selective channel $h^{(r)}[n;\, \theta]$ for $n \in \{i(N+c) + c + d - L' + 1, \ldots, (i+1)(N+c) + d\}$ as

$$h^{(r)}[n;\, \theta] = \sum_{l=0}^{L} \delta[\theta - l] \sum_{q=-Q/2}^{Q/2} h_{q,l}^{(r)}[i] \mathrm{e}^{\mathrm{j}2\pi qn/K} \tag{3}$$

where d is some synchronisation (decision) delay and L' is a constant greater than or equal to the channel order L. The coefficients $h_{q,l}^{(r)}[i]$ are kept constant over a period of $(N+L')T$. The parameter Q is the number of TV basis

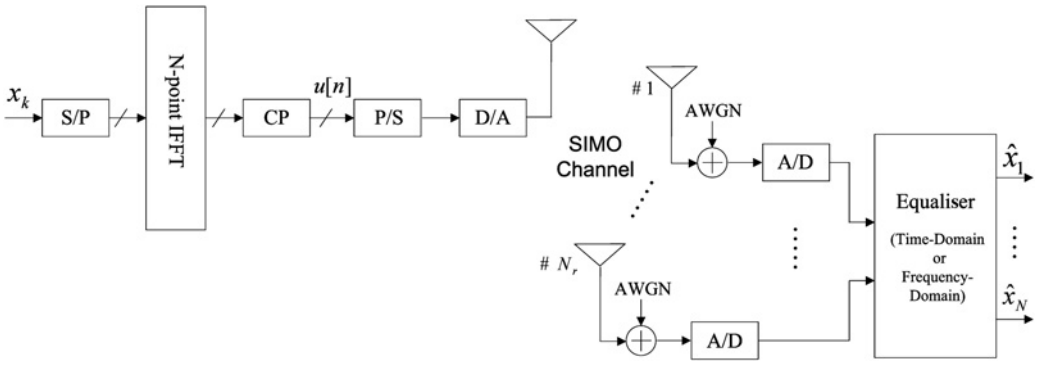

Figure 1 *SIMO-OFDM system model*

doi: 10.1049/iet-com.2008.0659

functions. K determines the BEM frequency resolution, and is assumed to be larger than or equal to the number of subcarriers, that is, $K \geq N$. In fact, the BEM is periodic with a period K. Therefore as the true channel is generally not periodic, K should at least be as large as N [24]. In addition, choosing $K = N$ leads to bordering effect that causes degradation in model accuracy [25]. In this study, it is assumed that the BEM frequency resolution K is an integer multiple of the FFT size, that is, $K = PN$, where P is an integer greater than or equal to 1. The number of TV basis functions Q should be selected such that $Q/(2KT) \geq f_{\max}$ [23]. Using the BEM, the received signal $y^{(r)}[n]$ can be written as

$$y^{(r)}[n] = \sum_{l=0}^{L} \sum_{q=-Q/2}^{Q/2} e^{j2\pi qn/K} h_{q,l}^{(r)}[i] u[n-l] + \xi^{(r)}[n] \quad (4)$$

Note that the definitions in (3) and (4) are approximations of the true channel and the received sequence, respectively. These equations are used only to simplify the derivation of the proposed equalisers, which are then used to equalise the true channel. Describing (4) in a block-based formulation, a block of N samples of the received sequence $y^{(r)}[n]$ can be shown as [19]

$$\boldsymbol{y}^{(r)}[i] = \underbrace{\sum_{q=-Q/2}^{Q/2} \boldsymbol{\Omega}_q[i] \left[\boldsymbol{O}_1, \boldsymbol{H}_q^{(r)}[i], \boldsymbol{O}_2\right] (\boldsymbol{I}_3 \otimes \boldsymbol{P})(\boldsymbol{I}_3 \otimes \boldsymbol{\mathcal{F}}^{\mathrm{H}})}_{\boldsymbol{G}^{(r)}[i]} \times \underbrace{\begin{bmatrix} \boldsymbol{x}[i-1] \\ \boldsymbol{x}[i] \\ \boldsymbol{x}[i+1] \end{bmatrix}}_{\tilde{\boldsymbol{x}}} + \boldsymbol{\xi}^{(r)}[i] = \boldsymbol{G}^{(r)}[i]\tilde{\boldsymbol{x}} + \boldsymbol{\xi}^{(r)}[i] \quad (5)$$

where i is the block index, $\boldsymbol{y}^{(r)}[i] = [y^{(r)}[i(N+c) + c + d + 1], \ldots, y^{(r)}[(i+1)(N+c) + d]]^{\mathrm{T}}$, $\boldsymbol{O}_1 = \boldsymbol{0}_{N\times(N+2c+d-L)}$, $\boldsymbol{O}_2 = \boldsymbol{0}_{N\times(N+c-d)}$, $\boldsymbol{\Omega}_q[i] = \mathrm{diag}[e^{j2\pi q(i(N+c)+c+d+1)/K}, \ldots, e^{j2\pi q((i+1)(N+c)+d)/K}]$, $\boldsymbol{x}[i] = [x_1[i], \ldots, x_N[i]]^{\mathrm{T}}$ and $\boldsymbol{\xi}^{(r)}[i] = [\xi^{(r)}[i(N+c) + c + d + 1], \ldots, \xi^{(r)}[(i+1)(N+c) + d]]^{\mathrm{T}}$. $\boldsymbol{H}_q^{(r)}[i]$ is an $N \times (N+L)$ Toeplitz matrix with first column $[h_{q,L}^{(r)}[i], \boldsymbol{0}_{1\times(N-1)}]^{\mathrm{T}}$ and first row $[h_{q,L}^{(r)}[i], \ldots, h_{q,0}^{(r)}[i], \boldsymbol{0}_{1\times(N-1)}]$ and $\boldsymbol{P}$ is the CP insertion matrix given by

$$\boldsymbol{P} = \begin{bmatrix} \boldsymbol{0}_{c\times(N-c)} & \boldsymbol{I}_c \\ & \boldsymbol{I}_N \end{bmatrix}$$

If there is no equalisation at the receiver, the demodulated signal in the frequency domain can be obtained by taking the FFT of sum of the N_r received sequences

$$\boldsymbol{y}_f[i] = \boldsymbol{\mathcal{F}}\left(\sum_{r=1}^{N_r} \boldsymbol{y}^{(r)}[i]\right) = \boldsymbol{\mathcal{F}}\left(\sum_{r=1}^{N_r} \boldsymbol{G}^{(r)}[i]\right)\tilde{\boldsymbol{x}} + \boldsymbol{\mathcal{F}}\left(\sum_{r=1}^{N_r} \boldsymbol{\xi}^{(r)}[i]\right) \quad (6)$$

The vector $\tilde{\boldsymbol{x}}$ in (6) can be rewritten as a linear combination of three successive transmitted blocks as follows

$$\tilde{\boldsymbol{x}} = \begin{bmatrix} \boldsymbol{x}[i-1] \\ \boldsymbol{x}[i] \\ \boldsymbol{x}[i+1] \end{bmatrix} = \begin{bmatrix} \boldsymbol{I}_N \\ \boldsymbol{0}_N \\ \boldsymbol{0}_N \end{bmatrix} \boldsymbol{x}[i-1] + \begin{bmatrix} \boldsymbol{0}_N \\ \boldsymbol{I}_N \\ \boldsymbol{0}_N \end{bmatrix} \boldsymbol{x}[i] + \begin{bmatrix} \boldsymbol{0}_N \\ \boldsymbol{0}_N \\ \boldsymbol{I}_N \end{bmatrix} \boldsymbol{x}[i+1] \triangleq \boldsymbol{E}_{-1}\boldsymbol{x}[i-1] + \boldsymbol{E}_0\boldsymbol{x}[i] + \boldsymbol{E}_1\boldsymbol{x}[i+1] \quad (7)$$

Substituting (7) into (6) yields

$$\boldsymbol{y}_f[i] = \underbrace{\boldsymbol{\mathcal{F}}\left(\sum_{r=1}^{N_r} \boldsymbol{G}^{(r)}[i]\right)\boldsymbol{E}_0}_{\boldsymbol{A}} \boldsymbol{x}[i] + \underbrace{\boldsymbol{\mathcal{F}}\left(\sum_{r=1}^{N_r} \boldsymbol{G}^{(r)}[i]\right)\boldsymbol{E}_{-1}}_{\boldsymbol{B}} \boldsymbol{x}[i-1] + \underbrace{\boldsymbol{\mathcal{F}}\left(\sum_{r=1}^{N_r} \boldsymbol{G}^{(r)}[i]\right)\boldsymbol{E}_1}_{\boldsymbol{C}} \boldsymbol{x}[i+1] + \underbrace{\boldsymbol{\mathcal{F}}\left(\sum_{r=1}^{N_r} \boldsymbol{\xi}^{(r)}[i]\right)}_{\boldsymbol{z}} \quad (8)$$

To focus on the received signal on kth carrier, the kth frequency component of the demodulated signal $\boldsymbol{y}_f[i]$ is expressed as

$$\boldsymbol{y}_{f,k}[i] = \boldsymbol{A}(k,k)\boldsymbol{x}_k[i] + \sum_{\substack{m=1 \\ m\neq k}}^{N} \boldsymbol{A}(k,m)\boldsymbol{x}_m[i] + \sum_{m=1}^{N} \boldsymbol{B}(k,m)\boldsymbol{x}_m[i-1] + \sum_{m=1}^{N} \boldsymbol{C}(k,m)\boldsymbol{x}_m[i+1] + \sum_{m=1}^{N} \boldsymbol{\mathcal{F}}(k,m)\boldsymbol{z}_m[i] \quad (9)$$

where $\boldsymbol{A}(k,k)\boldsymbol{x}_k[i]$ is the desired term free of interference, and the second term is the ICI component. The third and fourth terms are IBI contributions from the previous and the following blocks, respectively. The last term is additive noise. The SINR at the kth frequency bin is defined as

$$\mathrm{SINR}^{(k)} = P_{\mathrm{s}}^{(k)} / (P_{\mathrm{ICI}}^{(k)} + P_{\mathrm{IBI_p}}^{(k)} + P_{\mathrm{IBI_f}}^{(k)} + P_{\mathrm{noise}}^{(k)}) \quad (10)$$

where $P_{\mathrm{s}}^{(k)}$, $P_{\mathrm{ICI}}^{(k)}$, $P_{\mathrm{IBI_p}}^{(k)}$, $P_{\mathrm{IBI_f}}^{(k)}$ and $P_{\mathrm{noise}}^{(k)}$ represent the signal power, the ICI power, the IBI power resulted from the previous block, the IBI power of the following block and noise power, respectively. The different power terms are

derived as follows

$$P_{\mathrm{s}}^{(k)} = \mathcal{E}\{|\boldsymbol{A}(k,\,k)|^2\}\mathcal{E}\{|\boldsymbol{x}_k[i]|^2\}$$
$$= \sigma_x^2|\boldsymbol{A}(k,\,k)|^2 = \sigma_x^2|\boldsymbol{e}^{(k)\mathrm{H}}\boldsymbol{A}\boldsymbol{e}^{(k)}|^2$$
$$P_{\mathrm{ICI}}^{(k)} = \sum_{\substack{m=1\\m\neq k}}^{N}\mathcal{E}\{|\boldsymbol{A}(k,\,m)\boldsymbol{x}_m[i]|^2\} = \sigma_x^2\sum_{\substack{m=1\\m\neq k}}^{N}|\boldsymbol{e}^{(k)\mathrm{H}}\boldsymbol{A}\boldsymbol{e}^{(m)}|^2$$
$$P_{\mathrm{IBI_p}}^{(k)} = \sigma_x^2\sum_{m=1}^{N}|\boldsymbol{B}(k,\,m)|^2,\ P_{\mathrm{IBI_f}}^{(k)} = \sigma_x^2\sum_{m=1}^{N}|\boldsymbol{C}(k,\,m)|^2$$
$$P_{\mathrm{noise}}^{(k)} = \sum_{m=1}^{N}|\boldsymbol{\mathcal{F}}(k,\,m)|^2\mathcal{E}\{|\boldsymbol{z}_m[i]|^2\} \tag{11}$$

where $\boldsymbol{e}^{(k)}$ is the kth unit vector of size $N\times 1$, and the transmitted QPSK symbols are assumed to be i.i.d random variables, with equal variance σ_x^2. In the next section, this interference analysis is employed to design a TEQ.

3 Time-domain equalisation

In this section, a TEQ is proposed for SIMO-OFDM systems in doubly selective channels. The idea is to apply a block linear equaliser or filter $\boldsymbol{G}_e^{(r)}[i]$ on the rth receive antenna, as depicted in Fig. 2. Then, the sum of equaliser outputs is demodulated by FFT block to estimate the transmitted QPSK symbol on each tone. Hence, $\boldsymbol{x}[i]$ is estimated by $\hat{\boldsymbol{x}}[i]$ as

$$\hat{\boldsymbol{x}}[i] = \boldsymbol{\mathcal{F}}\left(\sum_{r=1}^{N_r}\boldsymbol{G}_e^{(r)}[i]\boldsymbol{y}'^{(r)}[i]\right) \tag{12}$$

where $\boldsymbol{y}'^{(r)}[i]$ is the input to the rth equaliser and contains $N+L'$ samples of the received signal $y^{(r)}[n]$ for $n\in\{i(N+c)+c+d-L'+1,\,\ldots,\,(i+1)(N+c)+d\}$. Similar to (5), $\boldsymbol{y}'^{(r)}[i]$ is described as

$$\boldsymbol{y}'^{(r)}[i] = \underbrace{\sum_{q=-Q/2}^{Q/2}\boldsymbol{\Omega}_q'[i]\left[\boldsymbol{O}_1',\boldsymbol{H}_q'^{(r)}[i],\boldsymbol{O}_2'\right](\boldsymbol{I}_3\otimes\boldsymbol{P})(\boldsymbol{I}_3\otimes\boldsymbol{\mathcal{F}}^{\mathrm{H}})}_{\boldsymbol{G}'^{(r)}[i]}$$
$$\times\tilde{\boldsymbol{x}}+\boldsymbol{\xi}'^{(r)}[i] = \boldsymbol{G}'^{(r)}[i]\tilde{\boldsymbol{x}}+\boldsymbol{\xi}'^{(r)}[i] \tag{13}$$

where $\boldsymbol{\Omega}_q'[i] = \mathrm{diag}\{[\mathrm{e}^{\mathrm{j}2\pi q(i(N+c)+c-L'+d+1)/K},\ldots,\mathrm{e}^{\mathrm{j}2\pi q((i+1)(N+c)+d)/K}]\}$, $\boldsymbol{O}_1' = \boldsymbol{0}_{(N+L')\times(N+2c+d-L-L')}$, $\boldsymbol{O}_2' = \boldsymbol{0}_{(N+L')\times(N+c-d)}$ and $\boldsymbol{H}_q'^{(r)}[i]$ is an $(N+L')\times(N+L+L')$ Toeplitz matrix with first column $[h_{q,L}^{(r)}[i],\boldsymbol{0}_{1\times(N+L'-1)}]^{\mathrm{T}}$ and first row $[h_{q,L}^{(r)}[i],\ldots,h_{q,0}^{(r)}[i],\boldsymbol{0}_{1\times(N+L'-1)}]$. Defining $\boldsymbol{G}_e[i] = [\boldsymbol{G}_e^{(1)}[i],\ldots,\boldsymbol{G}_e^{(N_r)}[i]]$, and $\boldsymbol{y}'[i] = [\boldsymbol{y}'^{(1)T}[i],\ldots,\boldsymbol{y}'^{(N_r)\mathrm{T}}[i]]^{\mathrm{T}}$, (12) is written as

$$\hat{\boldsymbol{x}}[i] = \boldsymbol{\mathcal{F}}\boldsymbol{G}_e[i]\boldsymbol{y}'[i] \tag{14}$$

The TEQ $\boldsymbol{G}_e[i]$ can be designed based on maximising the SINR. Using (13) and (14) and following the interference analysis procedure in Section 2, the signal, ICI, IBI and noise powers in the presence of TEQ are derived as

$$P_{\mathrm{s}}^{(k)} = \sigma_x^2\left(\sum_{r=1}^{N_r}\boldsymbol{g}_{ek}^{(r)\mathrm{H}}[i]\boldsymbol{g}_k^{(r)}[i]\times\sum_{r=1}^{N_r}\boldsymbol{g}_k^{(r)\mathrm{H}}[i]\boldsymbol{g}_{ek}^{(r)}[i]\right)$$
$$= \sigma_x^2\boldsymbol{g}_{ek}^{\mathrm{H}}[i]\boldsymbol{g}_k[i]\boldsymbol{g}_k^{\mathrm{H}}[i]\boldsymbol{g}_{ek}[i]$$
$$P_{\mathrm{ICI}}^{(k)} = \sigma_x^2\boldsymbol{g}_{ek}^{\mathrm{H}}[i]\boldsymbol{G}[i]\boldsymbol{E}_0\left(\boldsymbol{I}_N-\boldsymbol{e}^{(k)}\boldsymbol{e}^{(k)\mathrm{H}}\right)\boldsymbol{E}_0^{\mathrm{H}}\boldsymbol{G}^{\mathrm{H}}[i]\boldsymbol{g}_{ek}[i]$$
$$P_{\mathrm{IBI_p}}^{(k)} = \sigma_x^2\boldsymbol{g}_{ek}^{\mathrm{H}}[i]\boldsymbol{G}[i]\boldsymbol{E}_{-1}\boldsymbol{E}_{-1}^{\mathrm{H}}\boldsymbol{G}^{\mathrm{H}}[i]\boldsymbol{g}_{ek}[i]$$
$$P_{\mathrm{IBI_f}}^{(k)} = \sigma_x^2\boldsymbol{g}_{ek}^{\mathrm{H}}[i]\boldsymbol{G}[i]\boldsymbol{E}_1\boldsymbol{E}_1^{\mathrm{H}}\boldsymbol{G}^{\mathrm{H}}[i]\boldsymbol{g}_{ek}[i]$$
$$P_{\mathrm{noise}}^{(k)} = \frac{\sigma_\xi^2}{N}\mathrm{trace}\{\boldsymbol{G}_e[i]\boldsymbol{G}_e^{\mathrm{H}}[i]\} \tag{15}$$

where $\boldsymbol{g}_k^{(r)}[i]\triangleq\boldsymbol{G}'^{(r)}[i]\boldsymbol{E}_0\boldsymbol{e}^{(k)}$, $\boldsymbol{f}_k\triangleq\boldsymbol{\mathcal{F}}^{\mathrm{H}}\boldsymbol{e}^{(k)}$, $\boldsymbol{g}_{ek}^{(r)}[i]\triangleq\boldsymbol{G}_e^{(r)\mathrm{H}}[i]\boldsymbol{f}_k$, $\boldsymbol{g}_{ek}[i] = \left[\boldsymbol{g}_{ek}^{(1)\mathrm{T}}[i],\ldots,\boldsymbol{g}_{ek}^{(N_r)\mathrm{T}}[i]\right]^{\mathrm{T}}$, $\boldsymbol{g}_k[i] = \left[\boldsymbol{g}_k^{(1)\mathrm{T}}[i],\ldots,\boldsymbol{g}_k^{(N_r)\mathrm{T}}[i]\right]^{\mathrm{T}}$ and $\boldsymbol{G}[i] = \left[\boldsymbol{G}'^{(1)\mathrm{T}}[i],\ldots,\boldsymbol{G}'^{(N_r)\mathrm{T}}[i]\right]^{\mathrm{T}}$.

Assuming $\boldsymbol{g}_{ek}^{\mathrm{H}}[i]\boldsymbol{g}_{ek}[i]=1$ for $1\le k\le N$, which results in trace $\{\boldsymbol{G}_e[i]\,\boldsymbol{G}_e^{\mathrm{H}}[i]\} = N$; and substituting (15) into (10), the SINR at the kth frequency bin in the presence of TEQ is given by

$$\mathrm{SINR}^{(k)}[i] = \frac{\boldsymbol{g}_{ek}^{\mathrm{H}}[i]\boldsymbol{g}_k[i]\boldsymbol{g}_k^{\mathrm{H}}[i]\boldsymbol{g}_{ek}[i]}{\boldsymbol{g}_{ek}^{\mathrm{H}}[i]\left(\boldsymbol{R}_k[i]+(\sigma_\xi^2/\sigma_x^2)\boldsymbol{I}_N\right)\boldsymbol{g}_{ek}[i]} \tag{16}$$

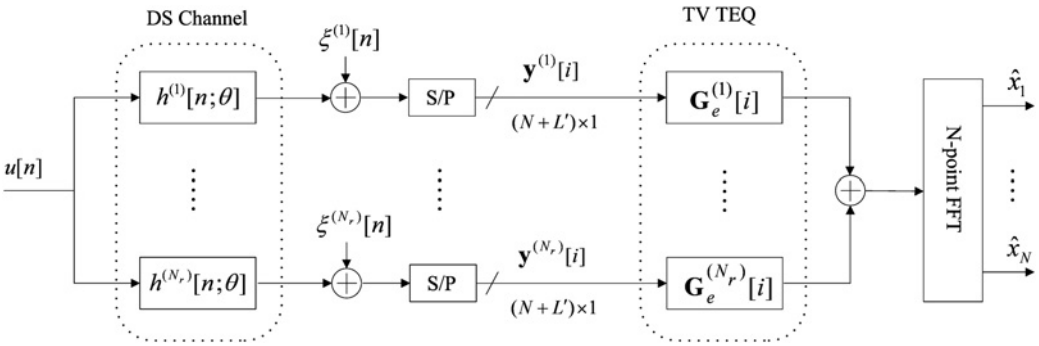

Figure 2 *Proposed time-domain equaliser (Prop-TEQ)*

doi: 10.1049/iet-com.2008.0659

where $\boldsymbol{R}_k[i] = \boldsymbol{G}[i](\boldsymbol{E}_0(\boldsymbol{I}_N - \boldsymbol{e}^{(k)}\boldsymbol{e}^{(k)\mathrm{H}})\boldsymbol{E}_0^{\mathrm{H}} + \boldsymbol{E}_{-1}\boldsymbol{E}_{-1}^{\mathrm{H}} + \boldsymbol{E}_1\,\boldsymbol{E}_1^{\mathrm{H}})\,\boldsymbol{G}^{\mathrm{H}}[i]$. Therefore TEQ is obtained by solving the following optimisation problem for $1 \le k \le N$

$$\max_{\boldsymbol{g}_{ek}[i]} \boldsymbol{g}_{ek}^{\mathrm{H}}[i]\boldsymbol{g}_k[i]\boldsymbol{g}_k^{\mathrm{H}}[i]\boldsymbol{g}_{ek}[i]$$

subject to

$$\boldsymbol{g}_{ek}^{\mathrm{H}}[i]\left(\boldsymbol{R}_k[i] + \frac{\sigma_\xi^2}{\sigma_x^2}\boldsymbol{I}_N\right)\boldsymbol{g}_{ek}[i] = 1$$

and

$$\boldsymbol{g}_{ek}^{\mathrm{H}}[i]\,\boldsymbol{g}_{ek}[i] = 1$$

This is a standard generalised eigenvalue problem and can be solved as follows [26]

(a) Compute $\boldsymbol{R}_{yy}[i] = \boldsymbol{G}[i]\left(\boldsymbol{E}_0\boldsymbol{E}_0^{\mathrm{H}} + \boldsymbol{E}_{-1}\boldsymbol{E}_{-1}^{\mathrm{H}} + \boldsymbol{E}_1^{\mathrm{H}}\boldsymbol{E}_1^{\mathrm{H}}\right)\times \boldsymbol{G}^{\mathrm{H}}[i] + (\sigma_\xi^2/\sigma_x^2)\boldsymbol{I}_{N+L'}$, and $\boldsymbol{R}_{yy}^{-1}[i]$.

(b) Compute the following for each k, $1 \le k \le N$:

- $\tilde{\boldsymbol{g}}_{ek}[i] = \boldsymbol{R}_{yy}^{-1}\boldsymbol{g}_k[i]$,
- $\boldsymbol{g}_{ek,\mathrm{opt}}[i] = \tilde{\boldsymbol{g}}_{ek}[i]/\|\tilde{\boldsymbol{g}}_{ek}[i]\|$.

Finally, the optimum equaliser is given by

$$\boldsymbol{G}_{e,\mathrm{opt}}[i] = \boldsymbol{\mathcal{F}}^{\mathrm{H}}\boldsymbol{G}_{ek,\mathrm{opt}}^{\mathrm{H}}[i] \tag{17}$$

where $\boldsymbol{G}_{ek,\mathrm{opt}}[i] = [\boldsymbol{g}_{e1,\mathrm{opt}}[i],\ \ldots,\boldsymbol{g}_{eN,\mathrm{opt}}[i]]$.

Note that the proposed TEQ, represented by Prop-TEQ, is optimal in the sense of maximising the total SINR at the output of the FFT demodulator. The proposed SINR formulation is exact since no simplifying assumption is used. This formulation, which is different from those found in literature, can be employed to maximise bit rate for a specified BER [27] or minimise the BER for a specified bit rate [28].

4 Per-tone frequency-domain equalisation

In Section 3, a TEQ was introduced to mitigate ICI and IBI in time- and frequency-selective channels. In this section a frequency-domain interference mitigation technique is proposed for SIMO-OFDM systems. This technique optimises the performance on each subcarrier separately.

For doubly selective channels, if the length of the CP is not less than the channel delay spread, IBI is completely eliminated, and only ICI occurs because of time variations of the channel. Traditional successive interference cancellation (SIC), MMSE and zero-forcing (ZF) equalisers for ICI suppression in [9, 29, 30], process N subcarrier signals simultaneously using all FFT output samples. Since the number of subcarriers is usually very large, these receivers have very high complexity. It has also been shown in [31, 32] that ICI power on each subcarrier is affected by only a few adjacent subcarriers. In other words, the desired subcarrier would be interfered by only a few neighbours. Accordingly, the computational complexity of the ICI equaliser can be significantly reduced without much sacrifice in performance. Based on the above fact, the transmitted symbol on the kth subcarrier can be estimated using a linear combination of the FFT output samples corresponding to that subcarrier and its neighbours. The linear combination for Q' neighbouring subcarriers and N_r received signals can be written as

$$\hat{x}_k[i] = \sum_{r=1}^{N_r}\sum_{q'=-Q'/2}^{Q'/2}\alpha_{q'}^{(r,k)}[i](\boldsymbol{\mathcal{F}}^{(k+q')}\boldsymbol{y}^{(r)}[i]) \tag{18}$$

The $\alpha_{q'}^{(r,k)}[i]$ coefficients can be obtained using MSE criterion. However, in the case of insufficient CP and doubly selective channel, IBI is present in addition to ICI and the above simple linear combination is no longer a good estimate of $x_k[i]$. In other words, each FFT output sample in (18) has some IBI from previous and next OFDM blocks. Hence, the ICI term in the kth FFT output cannot be estimated using a linear combination of adjacent subcarriers. To use (18) in the presence of both the ICI and IBI, one should obtain a method to remove IBI terms (explicitly or implicitly) from the FFT output samples. To remove IBI, $L'+1$ samples are required for each subcarrier where $L' \ge L$. In this paper, it is proposed to provide these samples through performing $L'+1$ FFT of size N on $N+L'$ received samples of each received signal path. This is equivalent to performing a sliding FFT on each of the incoming path signals. An IBI-free sample for each subcarrier can be obtained as a linear combination of the $L'+1$ outputs of the sliding FFT, corresponding to that subcarrier. The proposed IBI cancellation method can be used to extend (18) for joint ICI and IBI cancellation as follows

$$\hat{x}_k[i] = \sum_{r=1}^{N_r}\sum_{q'=-Q'/2}^{Q'/2}\alpha_{q'}^{(r,k)}[i]\{\boldsymbol{\beta}_{q'}^{(r,k)\mathrm{T}}[i](\tilde{\boldsymbol{\mathcal{F}}}^{(k+q')}\boldsymbol{y}'^{(r)}[i])\} \tag{19}$$

where $\boldsymbol{\beta}_{q'}^{(r,k)}[i] = [\beta_{q',0}^{(r,k)}[i],\ \ldots,\ \beta_{q',L'}^{(r,k)}[i]]^{\mathrm{T}}$

$$\tilde{\boldsymbol{\mathcal{F}}}^{(k)} = \begin{bmatrix} 0 & \ldots & 0 & \boldsymbol{\mathcal{F}}^{(k)} \\ \vdots & 0 & \boldsymbol{\mathcal{F}}^{(k)} & 0 \\ 0 & \iddots & 0 & \vdots \\ \boldsymbol{\mathcal{F}}^{(k)} & 0 & \ldots & 0 \end{bmatrix}$$

which represents a sliding FFT operation; and $\boldsymbol{y}'^{(r)}[i]$ is defined in (13).

Defining $\boldsymbol{w}_{q'}^{(r,k)\mathrm{T}} \triangleq \alpha_{q'}^{(r,k)}\boldsymbol{\beta}_{q'}^{(r,k)\mathrm{T}}$, (19) is written as

$$\hat{x}_k[i] = \sum_{r=1}^{N_r}\sum_{q'=-Q'/2}^{Q'/2} \boldsymbol{w}_{q'}^{(r,k)\mathrm{T}}[i]\tilde{\boldsymbol{\mathcal{F}}}^{(k+q')}\boldsymbol{y}'^{(r)}[i] \tag{20}$$

From (20), one can see that $x_k[i]$ is estimated through a linear combination of the sliding FFT output samples on the kth subcarrier and its Q' neighbours. A closed-matrix form representation is used to rewrite (20) as follows

$$\hat{x}_k[i] = \boldsymbol{w}^{(k)\mathrm{T}}[i](\boldsymbol{I}_{N_r} \otimes \tilde{\boldsymbol{F}}^{(k)})\boldsymbol{y}'[i] \tag{21}$$

where $\boldsymbol{w}_{q'}^{(r,k)}[i] = [w_{q',0}^{(r,k)}[i], \ldots, w_{q',L'}^{(r,k)}[i]]^{\mathrm{T}}$, $\boldsymbol{w}^{(r,k)}[i] = [\boldsymbol{w}_{-Q'/2}^{(r,k)\mathrm{T}}[i], \ldots, \boldsymbol{w}_{Q'/2}^{(r,k)\mathrm{T}}[i]]^{\mathrm{T}}$, $\boldsymbol{w}^{(k)}[i] = [\boldsymbol{w}^{(1,k)\mathrm{T}}[i], \ldots, \boldsymbol{w}^{(N_r,k)\mathrm{T}}[i]]^{\mathrm{T}}$, and $\tilde{\boldsymbol{F}}^{(k)} = [\tilde{\boldsymbol{\mathcal{F}}}^{(k-Q'/2)\mathrm{T}}, \ldots, \tilde{\boldsymbol{\mathcal{F}}}^{(k+Q'/2)\mathrm{T}}]^{\mathrm{T}}$.

Equation (21) indicates that each subcarrier (tone) has its own equaliser $\boldsymbol{w}^{(k)}[i]$ and thus, the equaliser coefficients can be optimised for each subcarrier separately. The PTEQ $\boldsymbol{w}^{(k)}[i]$ for the kth subcarrier is the solution of the following MMSE design criterion

$$\boldsymbol{w}^{(k)}[i] = \arg\min_{\boldsymbol{w}^{(k)}[i]} \mathcal{E}\left\{\left|x_k[i] - \boldsymbol{w}^{(k)\mathrm{T}}[i]\left(\boldsymbol{I}_{N_r} \otimes \tilde{\boldsymbol{F}}^{(k)}\right)\boldsymbol{y}'[i]\right|^2\right\} \tag{22}$$

Solving for $\boldsymbol{w}^{(k)}[i]$ in (22) yields

$$\begin{aligned}\boldsymbol{w}_{\mathrm{MMSE}}^{(k)*}[i] = {} & ((\boldsymbol{I}_{N_r} \otimes \tilde{\boldsymbol{F}}^{(k)})(\boldsymbol{G}[i]\boldsymbol{R}_{\tilde{\boldsymbol{x}}}\boldsymbol{G}^{\mathrm{H}}[i] + \boldsymbol{R}_{\boldsymbol{\xi}}) \\ & \times (\boldsymbol{I}_{N_r} \otimes \tilde{\boldsymbol{F}}^{(kH)}))^{-1} \times (\boldsymbol{I}_{N_r} \otimes \tilde{\boldsymbol{F}}^{(k)})\boldsymbol{G}[i]\boldsymbol{R}_{\tilde{\boldsymbol{x}}}\bar{\boldsymbol{e}}^{(k)}\end{aligned} \tag{23}$$

where $\bar{\boldsymbol{e}}^{(k)}$ is the $(3N) \times 1$ unit vector with a 1 in the position $N + k$. In this study, frequency-domain equalisers are represented as signal flow graphs (SFGs), building blocks of which are given in Fig. 3. The proposed per-tone equaliser (Prop-PTEQ) scheme for the kth subcarrier is depicted in Fig. 4. As shown in this figure, one sliding FFT is needed per receive antenna to compute (20). In the following, a low-complexity PTEQ is derived using a procedure similar to that of [33]. This procedure replaces the sliding FFT with only one full FFT and L' difference terms that are common to all subcarriers. Considering the

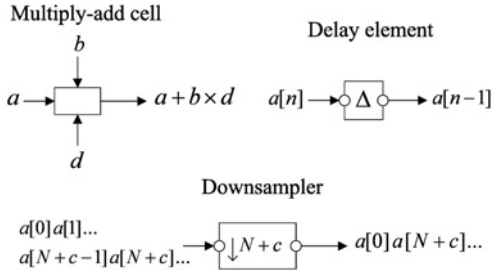

Figure 3 *Signal flow graph building blocks*

$(k + q')$th subcarrier of the sliding FFT in (20), it can be shown that

$$\tilde{\boldsymbol{\mathcal{F}}}^{(k+q')}\boldsymbol{y}'^{(r)}[i] = \boldsymbol{T}^{(k+q')}\begin{bmatrix} Y^{(r,k+q')} \\ \Delta\boldsymbol{y}'^{(r)}[i] \end{bmatrix} \tag{24}$$

where

$$\boldsymbol{T}^{(k+q')} = \begin{bmatrix} 1 & 0 & \cdots & 0 \\ \vartheta^{(k+q')} & \ddots & \ddots & \vdots \\ \vdots & \ddots & \ddots & 0 \\ \vartheta^{(k+q')L'} & \cdots & \vartheta^{(k+q')} & 1 \end{bmatrix}$$

with $\vartheta = \mathrm{e}^{-\mathrm{j}2\pi/N}$, and $Y^{(r,k+q')}$ is the FFT output sample on the $(k + q')$th subcarrier, which is computed as $Y^{(r,k+q')} = \boldsymbol{\mathcal{F}}^{(k+q')}[y^{(r)}[i(N + c) + c + d + 1], \ldots, y^{(r)}[(i + 1)(N + c) + d]]^{\mathrm{T}}$ and the difference terms $\Delta\boldsymbol{y}'^{(r)}[i]$ are

$$\Delta\boldsymbol{y}'^{(r)}[i] = \begin{bmatrix} y^{(r)}[i(N + c) + c + d] - \\ \qquad y^{(r)}[(i + 1)(N + c) + d] \\ \vdots \\ y^{(r)}[i(N + c) + c + d - L' + 1] - \\ \qquad y^{(r)}[(i + 1)(N + c) + d - L' + 1] \end{bmatrix}$$

Substituting (24) into (20) yields

$$\hat{x}_k[i] = \sum_{r=1}^{N_r}\sum_{q'=-Q'/2}^{Q'/2} \boldsymbol{w}_{q'^{(r,k)\mathrm{T}}}[i]\boldsymbol{T}^{(k+q')}\begin{bmatrix} Y^{(r,k+q')} \\ \Delta\boldsymbol{y}'^{(r)}[i] \end{bmatrix} \tag{25}$$

Define $\boldsymbol{v}_{q'(r,k)\mathrm{T}}[i] \triangleq \boldsymbol{w}_{q'}^{(r,k)\mathrm{T}}[i]\boldsymbol{T}^{(k+q')}$, $\boldsymbol{\gamma}_1^{(r,k)}[i] = [v_{-Q'/2,0}^{(r,k)}[i], \ldots, v_{Q'/2,0}^{(r,k)}[i]]^{\mathrm{T}}$, and $\boldsymbol{\gamma}_2^{(r,k)}[i] = [\sum_{q'=-Q'/2}^{Q'/2} v_{q',1}^{(r,k)}[i], \ldots, \sum_{q'=-Q'/2}^{Q'/2} v_{q',L'}^{(r,k)}[i]]^{\mathrm{T}}$ to rewrite (25) as follows

$$\begin{aligned}\hat{x}_k[i] &= \sum_{r=1}^{N_r}[\boldsymbol{\gamma}_1^{(r,k)\mathrm{T}}[i], \boldsymbol{\gamma}_2^{(r,k)\mathrm{T}}[i]] \times \begin{bmatrix} Y^{(r,k-Q'/2)} \\ \vdots \\ Y^{(r,k+Q'/2)} \\ \Delta\boldsymbol{y}'^{(r)}[i] \end{bmatrix} \\ &= \sum_{r=1}^{N_r}\boldsymbol{v}^{(r,k)\mathrm{T}}[i] \times \underbrace{\begin{bmatrix} \boldsymbol{0}_{1\times L'} & \boldsymbol{\mathcal{F}}^{(k-Q'/2)} & \\ \vdots & \vdots & \\ \boldsymbol{0}_{1\times L'} & \boldsymbol{\mathcal{F}}^{(k+Q'/2)} & \\ \bar{\boldsymbol{I}}_{L'} & \boldsymbol{0}_{L'\times(N-L')} & -\bar{\boldsymbol{I}}_{L'} \end{bmatrix}}_{\hat{\boldsymbol{F}}^{(k)}} \boldsymbol{y}'^{(r)}[i]\end{aligned} \tag{26}$$

where $\boldsymbol{v}^{(r,k)}[i] = [\boldsymbol{\gamma}_1^{(r,k)\mathrm{T}}[i], \boldsymbol{\gamma}_2^{(r,k)\mathrm{T}}[i]]^{\mathrm{T}}$ and $\bar{\boldsymbol{I}}_{L'}$ is the anti-diagonal identity matrix of size $L' \times L'$. Defining $\boldsymbol{v}^{(k)}[i] = [\boldsymbol{v}^{(1,k)\mathrm{T}}[i], \ldots, \boldsymbol{v}^{(N_r,k)\mathrm{T}}[i]]^{\mathrm{T}}$, (26) can finally be written as

$$\hat{x}_k[i] = \boldsymbol{v}^{(k)\mathrm{T}}[i](\boldsymbol{I}_{N_r} \otimes \hat{\boldsymbol{F}}^{(k)})\boldsymbol{y}'[i] \tag{27}$$

doi: 10.1049/iet-com.2008.0659

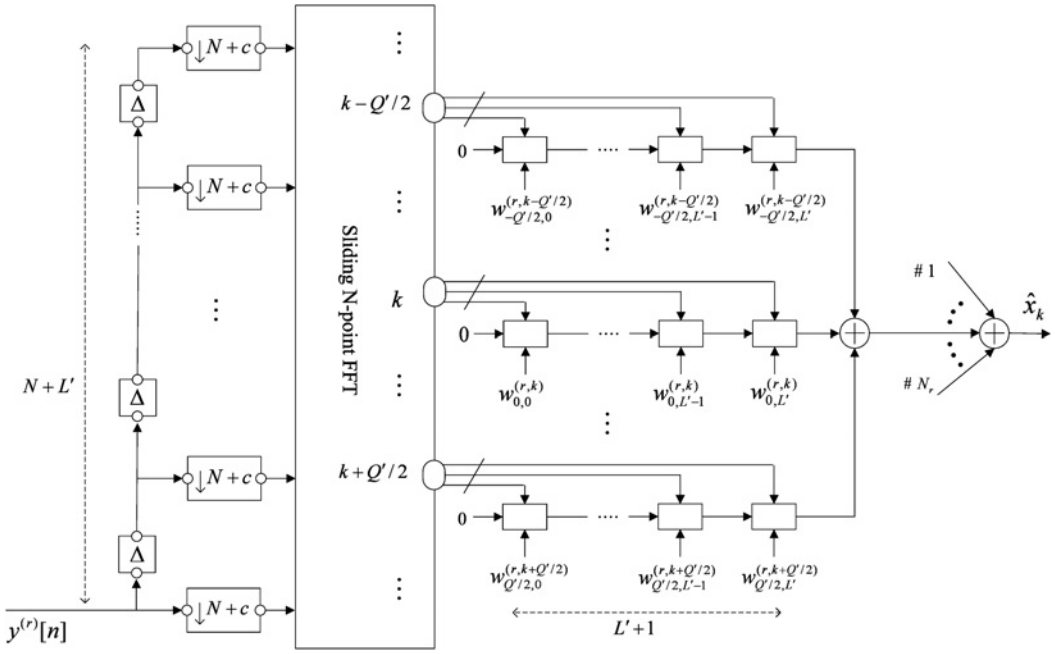

Figure 4 *Prop-PTEQ for the kth subcarrier*

Similar to (22), the MMSE PTEQ $\boldsymbol{v}^{(k)}[i]$ for the kth subcarrier is obtained by minimising the following cost function

$$\mathcal{J}[i] = \mathcal{E}\left\{\left|x_k[i] - \boldsymbol{v}^{(k)\mathrm{T}}[i]\left(\boldsymbol{I}_{N_r} \otimes \hat{\boldsymbol{F}}^{(k)}\right)\boldsymbol{y}'[i]\right|^2\right\} \quad (28)$$

Fig. 5 depicts the derived low-complexity PTEQ scheme for the kth subcarrier, denoted by Prop-LC-PTEQ.

5 Complexity comparison

In this section, the complexities of our proposed approaches are compared to those of recently proposed methods in [19] referred to as Imad-TEQ, Imad-PTEQ and Imad-LC-PTEQ. Two types of complexities can be distinguished: the design complexity and the implementation complexity. The design complexity is the complexity associated with computing the equaliser

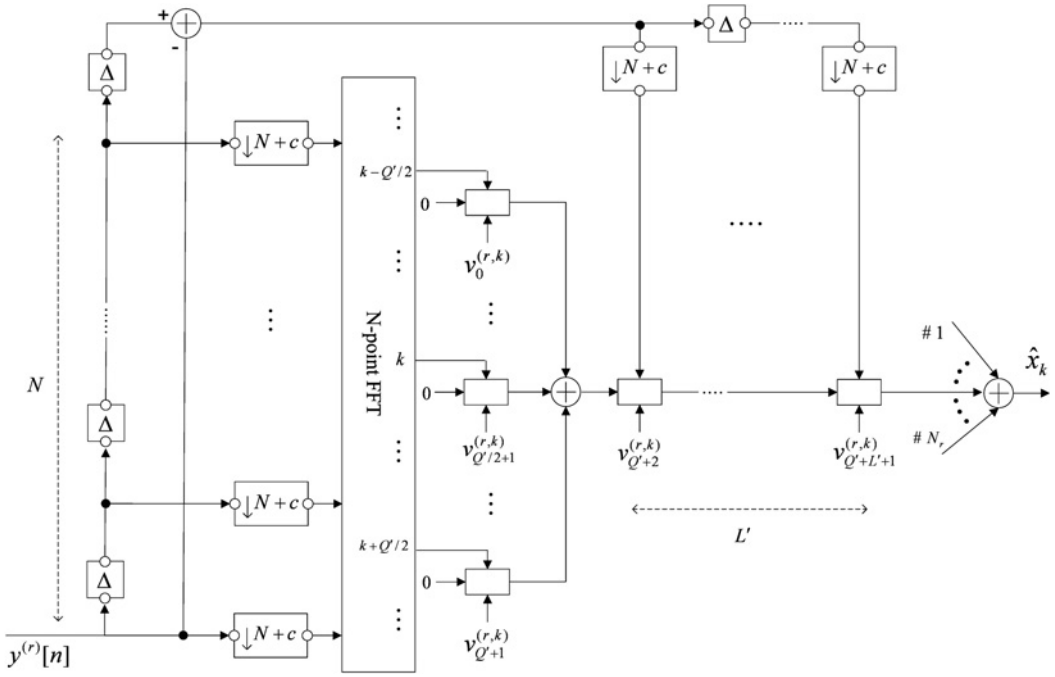

Figure 5 *Prop-LC-PTEQ for the kth subcarrier*

coefficients. The implementation complexity (run-time complexity) is the complexity associated with estimating a block of N QPSK symbols. The number of multiply-add (MA) operations are considered as a measure for complexity comparison.

5.1 Design complexity

The design complexity of proposed equalisers is summarised in Table 1. In this table, the design complexity of time and frequency-domain equalisers proposed in [19] is also shown. The design complexity of TEQs is mainly because of matrix inversion. If the channel is highly underspread ($LQ \ll N$) and L' and Q' are not much larger than L and Q, it may be assumed that $(L + L' + 1) \times (Q + Q' + 1)$ is less than $N + L'$, and thus the design complexity of the Prop-TEQ is higher than the design complexity of the Imad-TEQ. However, the performance of the Prop-TEQ is superior to that of Imad-TEQ (see Section 7). Furthermore, the design complexity of the Prop-TEQ can be reduced using a low-rank approximation of $\boldsymbol{R}_{yy}[i]$ (this technique has been used in [9] as part of the channel estimation process). From Table 1, it is seen that the design complexities of Prop-PTEQ and Imad-PTEQ are the same, whereas the design complexity of Prop-LC-PTEQ is less than that of the Imad-LC-PTEQ. Also, the design complexity of the Prop-LC-PTEQ is less than that of the Prop-TEQ.

5.2 Implementation complexity

Table 2 shows the implementation complexity of different equalisers. Again, for underspread channels, the implementation complexity of Prop-TEQ is higher than that of Imad-TEQ. However, as seen in Table 2, both Prop-PTEQ and Prop-PTEQ-LC have lower implementation complexities compared to frequency-domain equalisers in [19]. Furthermore, the implementation complexity of Prop-LC-PTEQ is lower than that of the Prop-TEQ.

Note that the results shown in the complexity tables are not valid for linear time-invariant (LTI) channels by setting $Q = 0$, since the circulant property of the channel can be exploited to perform low complexity matrix multiplication.

Table 1 Design complexity of different equalisers

Method	MA/rx
Imad-TEQ [19]	$\mathcal{O}((L + L' + 1)^3(Q + Q' + 1)^3)$/block
Prop-TEQ	$\mathcal{O}((N + L')^3)$/block
Imad-PTEQ [19]	$\mathcal{O}((Q' + 1)^2(L' + 1)^2 N)$/tone
Prop-PTEQ	$\mathcal{O}((Q' + 1)^2(L' + 1)^2 N)$/tone
Imad-LC-PTEQ [19]	$\mathcal{O}((PL' + Q' + 1)^2 P^2 N)$/tone
Prop-LC-PTEQ	$\mathcal{O}((L' + Q' + 1)^2 N)$/tone

LC denotes to low-complexity implementation of PTEQ

Table 2 Implementation complexity of different equalisers

Method	MA/tone/rx	FFT/rx
Imad-TEQ	$(Q' + 1)(L' + 1) + 1$	1
Prop-TEQ	$N + L'$	1
Imad-PTEQ	$(Q' + 1)(L' + 1)$	$(Q' + 1)$ sliding FFTs
Prop-PTEQ	$(Q' + 1)(L' + 1)$	1 sliding FFT
Imad-LC-PTEQ	$P(L' + 1) + Q' + 1$	P FFTs
Prop-LC-PTEQ	$L' + Q' + 1$	1

6 Unifying framework

In this section it is shown that the proposed frequency-domain technique in Section 4 unifies and extends several earlier results for both frequency and doubly selective channels.

(i) Frequency selective channels ($Q = 0$, and hence $Q' = 0$)

- $c \geq L$ and $L' = 0$: the proposed FEQ reduces to the one-tap MMSE FEQ as in [2];
- $c < L$ and $L' \neq 0$: the proposed FEQ reduces to the PTEQ proposed for discrete multitone transmission (DMT)-based systems in [34].

(ii) Doubly selective channels ($Q \neq 0$)

- $c \geq L$ and $L' = 0$, and $P = 1$: the proposed FEQ boils down to the frequency-domain equalisers proposed in [31, 35], and corresponds to the FEQ proposed in [36];
- $c < L$ and $L' \neq 0$, and $P = 1$: the proposed FEQ corresponds to the FEQ proposed in [19].

Note also that the proposed TEQ maximises a generalised Rayleigh quotient and hence fits into the unified framework for TEQs [37].

7 Simulations

In the following, numerical results are presented to demonstrate the effectiveness of the proposed methods. Other algorithms simulated in this section are one-tap MMSE [2] and Imad-PTEQ [19]. A SISO-OFDM system as well as a SIMO-OFDM system with two receive antennas are simulated. QPSK signalling and OFDM modulation with $N = 128$ subcarriers and a CP of length $c = 3$ is used. A doubly selective channel is simulated according to Jakes' model with $f_{\max} = 100$ Hz, and sampling time $T = 50\,\mu$s. Hence, the

doi: 10.1049/iet-com.2008.0659

normalised Doppler frequency is obtained as $f_{\max}T = 0.005$. The channel order is considered to be $L = 6$ and its autocorrelation function is given by $\mathcal{E}\{h^{(r_1)}[n_1; l_1]\, h^{(r_2)*}[n_2; l_2]\} = \sigma_l^2 J_0(2\pi f_{\max} T(n_1 - n_2))\delta[l_1 - l_2]\delta[r_1 - r_2]$, where J_0 is the zero-order Bessel function of the first kind and σ_l^2 is the lth tap power. In the simulations the channel is assumed to be wide sense stationary, uncorrelated scattering (WSSUS) with uniform power delay profile $\sigma_l^2 = \sigma_b^2$ for $l = 0, \ldots, L$. To design the equalisers, channel is modelled by BEM. The knowledge of the BEM coefficients of the channel is assumed at the receiver, and not the knowledge of the true Jakes' channel, which is rather difficult to obtain in practice. For the lth tap of the channel, in the ith OFDM block, the BEM coefficients vector $\boldsymbol{h}_l[i] = [h_{-Q/2,l}[i], \ldots, h_{Q/2,l}[i]]^{\mathrm{T}}$ is obtained by $\boldsymbol{h}_l[i] = \boldsymbol{\Psi}^{\dagger}[i]\boldsymbol{h}_l^{(\mathrm{jakes})}[i]$, where $\boldsymbol{h}_l^{(\mathrm{jakes})}[i] = [h_l^{(\mathrm{jakes})}[i(N + c) + c - L' + d + 1], \ldots h_l^{(\mathrm{jakes})}[(i + 1)(N + c) + d]]^{\mathrm{T}}$ is the lth tap of the TV channel over $N + L'$ QPSK symbol periods, and $\boldsymbol{\Psi}[i]$ is the $(N + L') \times (Q + 1)$ matrix with the $(q + Q/2 + 1)$th column given by $[e^{j2\pi q(i(N+c)+c-L'+d+1)/K}, \ldots, e^{j2\pi q((i+1)(N+c)+d)/K}]^{\mathrm{T}}$. In all simulations, the synchronisation (decision) delay is chosen to be $d = 3$. Performance will be assessed in terms of the BER against signal-to-noise ratio (SNR). The SNR is defined as follows

$$\mathrm{SNR} \triangleq \sigma_b^2(L + 1)\sigma_x^2/\sigma_\xi^2$$

Fig. 6 shows the average SINR gain resulting from the Prop-TEQ in both SISO- and SIMO-OFDM systems. The SINR gain is defined as

$$\mathrm{SINR\ gain}[i] \triangleq \left(\frac{\prod_{k=1}^{N} \mathrm{SINR}_{\mathrm{eq}}^{(k)}[i]}{\prod_{k=1}^{N} \mathrm{SINR}_{\mathrm{ueq}}^{(k)}[i]}\right)^{1/N}$$

where $\mathrm{SINR}_{\mathrm{eq}}^{(k)}[i]$($\mathrm{SINR}_{\mathrm{ueq}}^{(k)}[i]$) being the SINR at the kth subcarrier of the ith OFDM block with (or without) the Prop-TEQ. The SINR metric expresses the SINR improvement over all subcarriers. Fig. 6 depicts for various values of SNR, the average SINR gain achieved with critically sampled ($P = 1$) and oversampled ($P = 2$) BEM. For smaller values of the SNR, the SINR improvement is smaller, as Prop-TEQ attempts to suppress both ICI/IBI and additive noise. As SNR increases, the SINR improvement increases since the equaliser attempts to suppress (essentially) only IBI and ICI. It can also be seen that the oversampled BEM ($P = 2$) results in higher SINR improvement over all ranges of SNR. Moreover, as SNR increases, the difference between SINR gains for $P = 1$ and $P = 2$ increases considerably. From this figure it is evident that interference cancellation is greatly improved for $N_r = 2$ receive antennas over $N_r = 1$.

Fig. 7 compares the BER performance of different approaches for SISO-OFDM system. It is seen that the one-tap MMSE equaliser has failed to compensate for the doubly selective fading distortion. When $P = 1$, Prop-TEQ and Prop-PTEQ considerably outperform the one-tap MMSE, however, they suffer from an early error floor. This is due to mismatch between the BEM and true channel. Note that when $P = 1$, Prop-PTEQ corresponds to Imad-PTEQ, hence they have the same performance. In this figure it is also shown that the performance of the proposed equalisers is significantly improved using $P = 2$ over $P = 1$. When $P = 2$, Prop-PTEQ closely coincides with the performance of Imad-PTEQ. In this case, Prop-TEQ exhibits the same BER performance as Imad-PTEQ for SNR < 12 dB, however, increasing the SNR improves the performance of Prop-TEQ over both Prop-PTEQ and Imad-PTEQ. Comparing the results of Fig. 7 with the results reported in [19], it is evident that the Prop-TEQ significantly outperforms Imad-TEQ as well.

Fig. 8 illustrates the BER performance of different equalisers for SIMO-OFDM system with $N_r = 2$ receiving

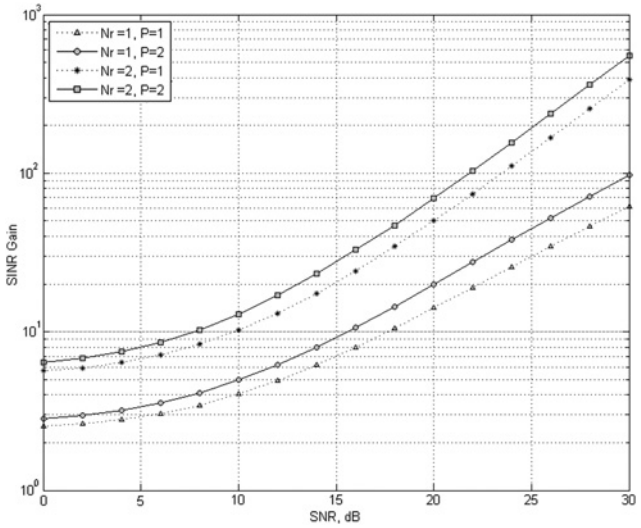

Figure 6 *SINR gain for Prop-TEQ*

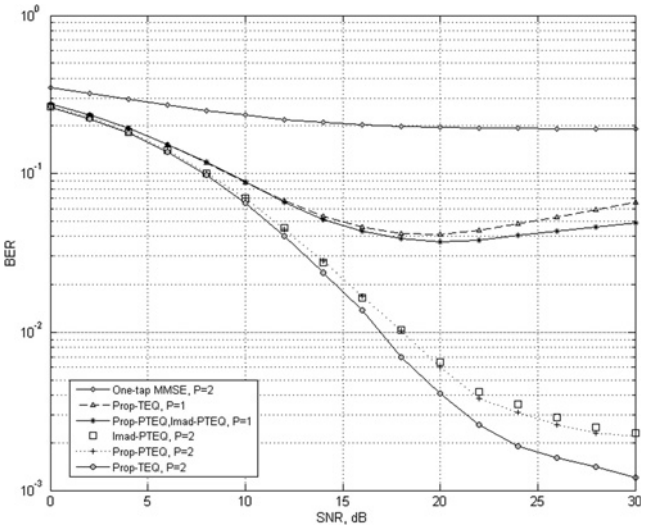

Figure 7 *BER comparison for SISO-OFDM system ($N_r = 1$)*

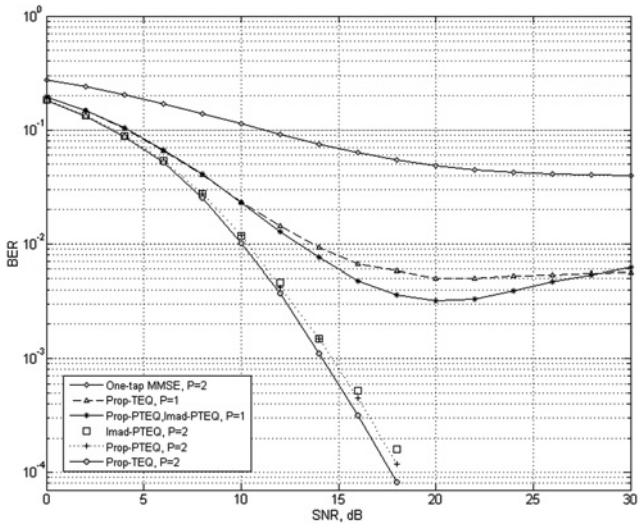

Figure 8 *BER comparison for SIMO-OFDM system ($N_r = 2$)*

antennas. Comparing Figs. 7 and 8 indicates that using $N_r > 1$ receiving antennas can lead to superior performances. Fig. 8 displays that similar to SISO case, one-tap MMSE cannot mitigate the interference well. For $P = 1$, Prop-TEQ and Prop-PTEQ show similar performances, however they suffer from an early error floor at BER 5×10^{-3} ($SNR = 20$ dB) and 3.2×10^{-3} (SNR = 20 dB), respectively. From Fig. 8, it is also observed that when $P = 2$, both proposed methods show significant improvement in BER performance. In this case, Prop-PTEQ closely follows the performance of Imad-PTEQ. In addition, Prop-TEQ performs as well as or better than both the Prop-PTEQ and Imad-PTEQ. As explained before, the Prop-LC-PTEQ and Imad-LC-PTEQ are derived by replacing the sliding FFT with only one full FFT and L' difference terms that are common to all subcarriers. In this approach no approximation is made and

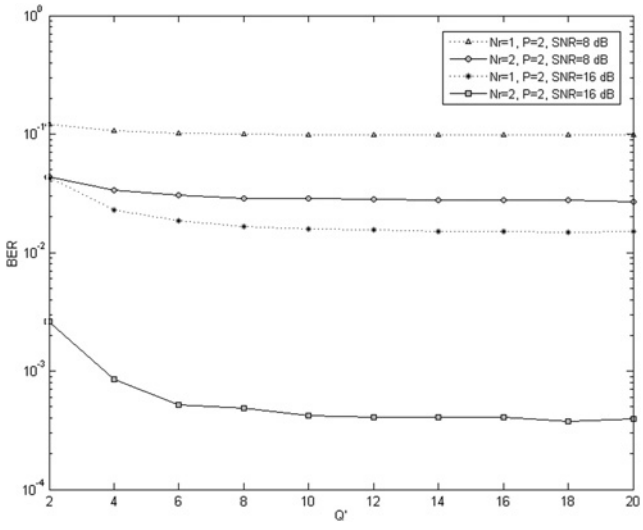

Figure 9 *BER against number of neighbouring subcarriers for Prop-PTEQ*

the functionality and performance of the low complexity variants of both equalisers remain unchanged. Hence, the performance comparison results for Prop-PTEQ and Imad-PTEQ (Figs. 7 and 8) are also valid for Prop-LC-PTEQ and Imad-LC-PTEQ.

Fig. 9 shows the performance of the proposed frequency-domain equaliser as a function of Q' (the number of dominant neighbouring subcarriers) at fixed SNR values of 8 and 16 dB for SISO and SIMO-OFDM systems. It is seen that a significant gain can be obtained by increasing Q' up to a certain threshold value after which, almost no gain is obtained. This justifies the choice of $Q' = 8$ in the previous simulations.

8 Conclusion

Two novel methods for equalisation of SIMO-OFDM systems over doubly selective channels considering the general case of insufficient CP and channel time variations are proposed. The time-domain equaliser, Prop-TEQ, is based on SINR maximisation and the per-tone frequency-domain equaliser, Prop-PTEQ, is based on MSE minimisation. An efficient low-complexity implementation is also developed for the per-tone approach.

The Prop-TEQ relies on a new exact SINR formulation and is actually designed in the frequency domain. This fact improves its performance considerably, compared to those of most of previously proposed TEQs [19, 37]. An interesting feature of the Prop-PTEQ is that it unifies and extends several earlier methods for both frequency selective and doubly selective channels. Also, the Prop-TEQ fits into the unified framework for TEQs [37].

Our simulations show that the proposed approaches substantially outperform the conventional one-tap MMSE equaliser [2]. It is also observed that the BEM frequency resolution has an important role in the performance of proposed equalisers and choosing the BEM frequency resolution equal to twice that of the FFT, leads to a significant performance improvement. In this case, Prop-PTEQ illustrates the same BER performance as Imad-PTEQ [19] with less complexity. In addition, it is shown that Prop-TEQ performs as well as or better than both the Prop-PTEQ and Imad-PTEQ. Finally, using multiple receive antennas may lead to superior performances.

9 References

[1] CIMINI JR. L.J.: 'Analysis and simulation of a digital mobile radio channel using orthogonal frequency division multiplexing', *IEEE Trans. Commun.*, 1985, **33**, (7), pp. 665–765

[2] WANG Z., GIANNAKIS G.B.: 'Wireless multicarrier communications: where Fourier meets Shannon', *IEEE Signal Process. Mag.*, 2000, **17**, (3), pp. 29–48

doi: 10.1049/iet-com.2008.0659

[3] AHSON S., ILYAS M.: 'WiMAX: technologies, performance analysis, and QoS' (CRC Press, 2007, 1st edn.)

[4] MOLISCH A.F., TOELTSCH M., VERMANI S.: 'Iterative methods for cancellation of intercarrier interference in OFDM systems', *IEEE Trans. Veh. Technol.*, 2007, **56**, (4), pp. 2158–2167

[5] KIM D., STUBER G.L.: 'Residual ISI cancellation for OFDM with applications to HDTV broadcasting', *IEEE J. Sel. Areas Commun.*, 1998, **16**, (8), pp. 1590–1599

[6] KIM J., KANG J., POWERS E.J.: 'A bandwidth efficient OFDM transmission scheme'. Proc. IEEE Int. Conf. Acoustics, Speech, Signal Processing, Washington, USA, May 2002, pp. 2329–2332

[7] ZHANG J., SER W., ZHU J.: 'Effective optimisation method for channel shortening in OFDM systems', *Proc. IEE Inst. Electr. Eng.-Commun.*, 2003, **150**, (2), pp. 85–90

[8] SCHNITER P.: 'Low-complexity equalization of OFDM in doubly selective channels', *IEEE Trans. Signal Process.*, 2004, **52**, (4), pp. 1002–1011

[9] CHOI Y.-S., VOLTZ P.J., CASSARA F.A.: 'On channel estimation and detection for multicarrier signals in fast and selective Rayleigh fading channels', *IEEE Trans. Commun.*, 2001, **49**, (8), pp. 1375–1387

[10] JEON W.G., CHANG K.H., CHO Y.S.: 'An equalization technique for orthogonal frequency division multiplexing systems in time-variant multipath channels', *IEEE Trans. Commun.*, 1999, **47**, (1), pp. 27–32

[11] CAI X., GIANNAKIS G.B.: 'Low-complexity ICI suppression for OFDM over time- and frequency-selective Rayleigh fading channels'. Proc. 36th Asilomar Conf. Signals, Systems, Computers, Pacific Grove, CA, November 2002, pp. 1822–1826

[12] WANG H., CHEN X., ZHOU S., ZHAO M., YAO Y.: 'Low-complexity ICI cancellation in frequency domain for OFDM systems in time-varying multipath channels', *IEICE Trans. Commun.*, 2006, **E89-B**, (3), pp. 1020–1023

[13] LEE H., KANG J., POWERS E.J.: 'Adaptive linear symbol detection for OFDM systems in time-frequency-selective fading channels', *IEICE Trans. Commun.*, 2007, **E90-B**, (3), pp. 685–688

[14] ARMSTRONG J.: 'Analysis of new and existing methods of reducing intercarrier interference due to carrier frequency offset in OFDM', *IEEE Trans. Commun.*, 1999, **47**, (3), pp. 365–369

[15] CHANG M.-X.: 'A novel algorithm of inter-subchannel interference self-cancellation for OFDM systems', *IEEE Trans. Wirel. commun.*, 2007, **6**, (8), pp. 2881–2893

[16] TRAUTMANN S., KARP T., FLIEGE N.J.: 'Frequency-domain equalization of DMT/OFDM systems with insufficient guard interval'. Proc. IEEE Int. Conf. Communication, New York, USA, April 2002, pp. 1646–1650

[17] PARK C.J., IM G.H.: 'Efficient DMT/OFDM transmission with insufficient cyclic prefix', *IEEE Commun. Lett.*, 2004, **8**, (9), pp. 576–578

[18] MA X., GIANNAKIS G.B., OHNO S.: 'Optimal training for block transmissions over doubly selective fading channels', *IEEE Trans. Signal Process.*, 2003, **51**, (5), pp. 1351–1366

[19] BARHUMI I., LEUS G., MOONEN M.: 'Equalization for OFDM over doubly selective channels', *IEEE Trans. Signal Process.*, 2006, **54**, (4), pp. 1445–1458

[20] TSATSANIS M.K., GIANNAKIS G.B.: 'Modeling and equalization of rapidly fading channels', *Int. J. Adaptive Control. Signal Process.*, 1996, **10**, (2/3), pp. 159–176

[21] SAYEED A.M., AAZHANG B.: 'Joint multipath-Doppler diversity in mobile wireless communications', *IEEE Trans. Commun.*, 1999, **47**, (1), pp. 123–132

[22] MARTONE M.: 'Wavelet-based separating kernels for array processing of cellular DS/CDMA signal in fast fading', *IEEE Trans. Commun.*, 2000, **48**, (1), pp. 979–995

[23] LEUS G., ZHOU S., GIANNAKIS G.B.: 'Orthogonal multiple access over time- and frequency-selective fading', *IEEE Trans. Inf. Theory*, 2003, **49**, (8), pp. 1942–1950

[24] ROUSSEAUX O., LEUS G., MOONEN M.: 'Estimation and equalization of doubly selective channels using known symbol padding', *IEEE Trans. Signal Process.*, 2006, **54**, (3), pp. 979–990

[25] CUI T., TELLAMBURA C., WU Y.: 'Low-complexity pilot-aided channel estimation for OFDM systems over doubly selective channels'. Proc. IEEE Int. Conf. Communications, Seoul, Korea, May 2005, pp. 1980–1984

[26] STAMOULIS A., DIGGAVI S.N., AL-DHAHIR N.: 'Intercarrier interference in MIMO OFDM', *IEEE Trans. Signal Process.*, 2002, **50**, (10), pp. 2451–2464

[27] VANBLEU K., YSEBAERT G., CUYPERS G., MOONEN M., VAN ACKER K.: 'Bitrate-maximizing time-domain equalizer design for DMT-based systems', *IEEE Trans. Commun.*, 2004, **52**, (6), pp. 871–876

[28] MARTIN R.K., YSEBAERT G., VANBLEU K.: 'Bit error rate minimizing channel shortening equalizers for cyclic prefixed systems', *IEEE Trans. Commun.*, 2007, **55**, (6), pp. 2605–2616

[29] YEH Y.-H., CHEN S.-G.: 'Reduction of Doppler-induced ICI by interference prediction'. Proc. IEEE Int. Symp. Pers., Indoor Mobile Radio Communication, Barcelona, Spain, September 2004, pp. 653–657

[30] LI G., YANG H., CAI L., GUI L.: 'A low-complexity equalization technique for OFDM system in time-variant multipath channels'. Proc. IEEE Veh. Technol. Conf., Orlando Florida, USA, October 2003, pp. 2466–2470

[31] CAI X.D., GIANNAKIS G.B.: 'Bounding performance and suppressing intercarrier interfenence in wireless mobile OFDM', *IEEE Trans. Commun.*, 2003, **51**, (12), pp. 2047–2056

[32] HUANG X., WU H.-C.: 'Intercarrier interference analysis for wireless OFDM in mobile channels'. Proc. IEEE Wireless Commun. Netw. Conf., Las Vegas, NV, USA, April 2006, pp. 1848–1853

[33] FARHANG-BOROUJENY B., GAZOR S.: 'Generalized sliding FFT and its application to implementation of block LMS adaptive filters', *IEEE Trans. Signal Process.*, 1994, **42**, (3), pp. 532–538

[34] VAN ACKER K., LEUS G., MOONEN M., VAN DEWIEL O., POLLET T.: 'Per-tone equalization for DMT-based systems', *IEEE Trans. Commun.*, 2001, **49**, (1), pp. 109–119

[35] HUANG X., WU H.-C.: 'Robust and efficient intercarrier interference mitigation for OFDM systems in time-varying fading channels', *IEEE Trans. Veh. Technol.*, 2007, **56**, (5), pp. 2517–1528

[36] BARHUMI I., LEUS G., MOONEN M.: 'Frequency-domain equalization for OFDM over doubly selective channels'. Proc. sixth Baiona Workshop Signal Processing and Communication, Baiona, Spain, 2003, pp. 103–107

[37] MARTIN R.K., VANBLEU K., DING M., YSEBAERT G., MILOSEVIC M., EVANS B.L., MOONEN M., JOHNSON C.R.: 'Unification and evaluation of equalization structures and design algorithms for discrete multitone modulation systems', *IEEE Trans. Signal Process.*, 2005, **53**, (10), pp. 3880–3894

doi: 10.1049/iet-com.2008.0659